AGU PUBLICATIONS

Geophysical Research Letters

RESEARCH LETTER
10.1002/2014GL060625

Key Points:
- Unforced decadal changes in global temperature are enhanced by TOA imbalances
- The Earth system tends to gain (lose) energy during warming (cooling) decades
- Albedo change associated with the IPO temporarily offsets the OLR response

Supporting Information:
- Readme
- Table S1 and Figures S1–S7

Correspondence to:
P. T. Brown,
Patrick.Brown@duke.edu

Citation:
Brown, P. T., W. Li, L. Li, and Y. Ming (2014), Top-of-atmosphere radiative contribution to unforced decadal global temperature variability in climate models, *Geophys. Res. Lett.*, *41*, 5175–5183, doi:10.1002/2014GL060625.

Received 22 MAY 2014
Accepted 8 JUL 2014
Accepted article online 10 July 2014
Published online 22 JUL 2014

Top-of-atmosphere radiative contribution to unforced decadal global temperature variability in climate models

Patrick T. Brown[1], Wenhong Li[1], Laifang Li[1], and Yi Ming[2]

[1]Earth and Ocean Sciences, Nicholas School of the Environment, Duke University, Durham, North Carolina, USA, [2]Geophysical Fluid Dynamics Laboratory/NOAA, Princeton University, Princeton, New Jersey, USA

Abstract Much recent work has focused on unforced global mean surface air temperature (*T*) variability associated with the efficiency of heat transport into the deep ocean. Here the relationship between unforced variability in *T* and the Earth's top-of-atmosphere (TOA) energy balance is explored in preindustrial control runs of the Coupled Model Intercomparison Project Phase 5 multimodel ensemble. It is found that large decadal scale variations in *T* tend to be significantly enhanced by the net energy flux at the TOA. This indicates that unforced decadal variability in *T* is not only caused by a redistribution of heat within the climate system but can also be associated with unforced changes in the total amount of heat in the climate system. It is found that the net TOA radiation imbalances result mostly from changes in albedo associated with the Interdecadal Pacific Oscillation that temporarily counteracts the climate system's outgoing longwave (i.e., Stefan-Boltzmann) response to *T* change.

1. Introduction

Global mean surface air temperature (*T*) is one of the most recognized metrics for assessing contemporary climate change and the impact of human activities on the planet. Therefore, decadal scale changes in the rate of increase of *T* are of great interest to the general public, policy makers, and scientists alike.

T change can be caused by external radiative forcings (*F*) which are imposed on the ocean-atmosphere system and have generally been defined to include anthropogenic alterations such as changes in greenhouse gas concentrations, sulfate aerosols, and land use albedo (among others), as well as natural influences such as changes in solar irradiance and volcanic aerosol concentration [*Solomon et al.*, 2007]. In addition to responding to the external radiative forcings, the climate system can produce unforced changes in *T* that spontaneously emerge from the ocean-atmosphere system's internal dynamics [*Hasselmann*, 1976; *Hawkins and Sutton*, 2009; *Meehl et al.*, 2009].

A slowdown in the rate of *T* warming in the early 21st century [*Trenberth and Fasullo*, 2013] has increased interest in unforced decadal *T* variability within the scientific community. Recent studies have mostly focused on unforced *T* variability associated with the efficiency of heat transport into the deep ocean [*Balmaseda et al.*, 2013; *England et al.*, 2014; *Guemas et al.*, 2013; *Meehl et al.*, 2011; *Meehl et al.*, 2013; *Trenberth and Fasullo*, 2013]. This type of unforced *T* variability results primarily from a change in the *distribution of heat* within the climate system. However, unforced variability can also work to alter the net energy balance at the top of the atmosphere (Q_{TOA}) via internal changes in clouds, water vapor, lapse rate, and/or sea ice, which could affect *T* and the *total amount of heat* in the climate system [*Palmer and McNeall*, 2014; *Trenberth et al.*, 2014]. The latter type of unforced variability has been studied at the interannual timescale [*Kato*, 2009; *Loeb et al.*, 2012; *Susskind et al.*, 2012; *Trenberth and Fasullo*, 2012], but there has been little work done at the decadal timescale, primarily because the best available satellite record, the Clouds and the Earth's Radiant Energy System [*Wielicki et al.*, 1996], is only ~13 years in length.

In the present study we utilize 36 preindustrial control runs (2400 months, deseasonalized) from the Coupled Model Intercomparison Project Phase 5 (CMIP5) multimodel ensemble [*Taylor et al.*, 2011] to assess the relative influence of decadal Q_{TOA} variability on *T* and to shed light on the physical processes primarily responsible for decadal Q_{TOA} variability.

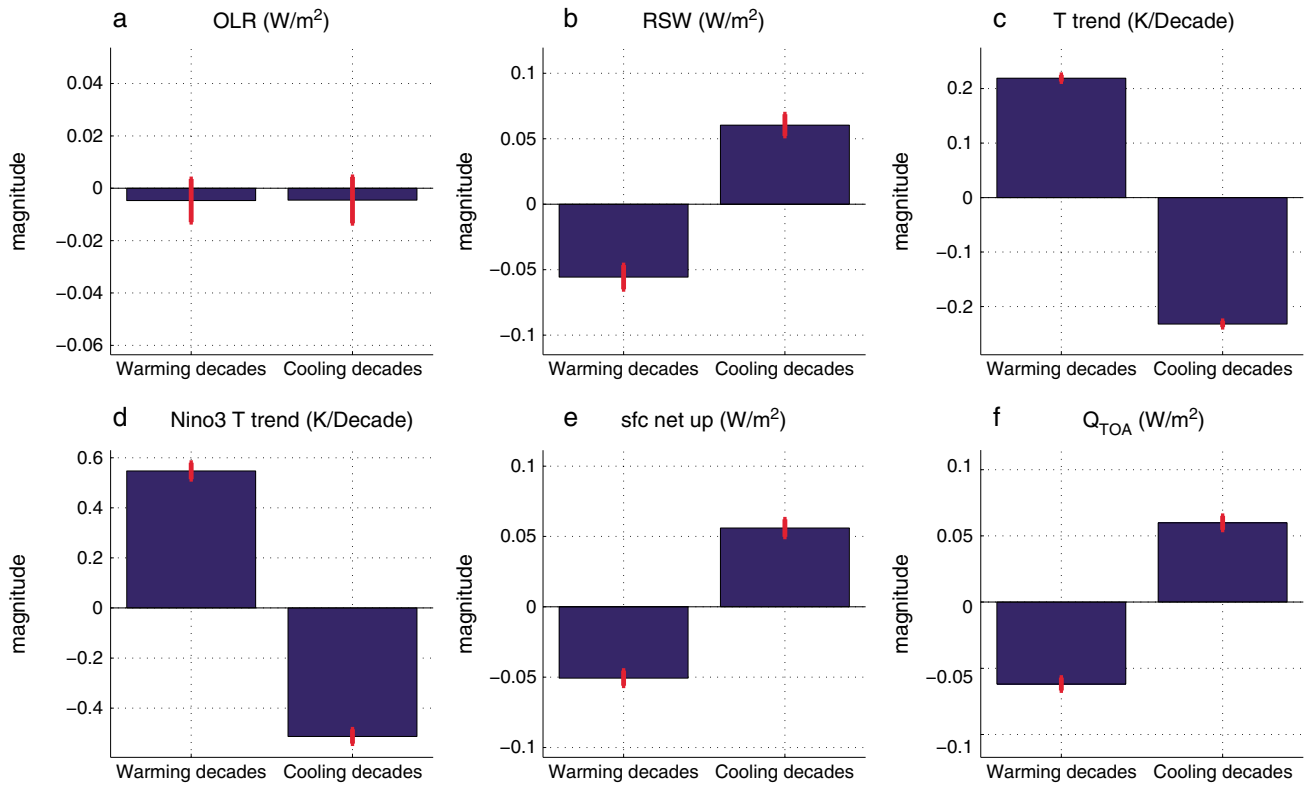

Figure 1. (a–f) Global magnitude (either linear trend or mean flux as indicated in the panels) of temperature and energy variables over warming and cooling decades (OLR: outgoing longwave radiation, RSW: reflected shortwave radiation, *T* trend: rate of change of global mean surface temperature, Niño 3 *T* trend: rate of change of surface air temperature over the Niño 3 region, sfc net up: upward oriented net surface energy flux, Q_{TOA}: upward oriented net TOA energy flux). The values of the two decades with the largest magnitude of *T* warming and the two decades with the largest magnitude of *T* cooling from each of the 36 CMIP5 GCM unforced control runs were incorporated into the average. Error bars represent standard errors across the 72 values (36 control runs multiplied by two warming/cooling decades per run). Similar results are obtained when more than two decades are chosen from each control run but the magnitude of the values decreases with increased decade number.

2. Conceptual Framework

In this work we utilize a common energy balance model to make a first-order quantification of the effect of unforced Q_{TOA} on decadal *T* change in CMIP5 models. In this framework, *T* change results from an energy imbalance (Q_{net}) on the coupled system composed of the Earth's land/atmosphere plus the upper ocean's mixed layer [*Baker and Roe*, 2009; *Dickinson*, 1981; *Geoffroy et al*., 2012; *Held et al*., 2010; *Wigley and Raper*, 1990; *Wigley and Schlesinger*, 1985]. An energy imbalance can be created at this system's upper boundary, via changes in the Earth's top-of-atmosphere net radiative energy budget (Q_{TOA}, positive upward) and/or it can be created at the system's lower boundary, via the redistribution of heat vertically across the bottom of the ocean's mixed layer (Q_{BML}, positive upward),

$$C_m \frac{dT}{dt} = Q_{net} = Q_{BML} - Q_{TOA}, \quad (1)$$

where C_m is the effective heat capacity of the system and depends mostly on the depth of the ocean's mixed layer (see supporting information).

For centennial timescales, Q_{BML} is typically represented as a simple diffusive process [*Baker and Roe*, 2009; *Geoffroy et al*., 2012; *Held et al*., 2010; *Wigley and Raper*, 1990; *Wigley and Schlesinger*, 1985] and can be thought of as a negative feedback on forced *T* change [*Baker and Roe*, 2009]. However, on the decadal timescale, unforced changes in vertical entrainment and Ekman pumping are also important components of Q_{BML} [*Deser et al*., 2010] and Q_{BML} flux can actively cause both positive and negative *T* change rather than simply acting as a negative feedback.

A linear decomposition of the full top-of-atmosphere (TOA) energy budget is $Q_{TOA} = -F + \lambda\Delta T - \varepsilon$, where F represents external radiative forcings, λ is the climate feedback parameter, $\lambda\Delta T$ represents the effects of fast feedbacks (clouds, ice albedo, water vapor, and lapse rate), and ε is spontaneous variability in the TOA radiation budget that is not caused by T change or external radiative forcing [*Forster and Gregory*, 2006; *Trenberth et al*., 2010]. In this study we utilize unforced control runs in which $F = 0$ and thus,

$$Q_{TOA} = \lambda\Delta T - \varepsilon. \tag{2}$$

Therefore, the unforced Q_{TOA} imbalances studied here are often themselves the *result* of T change (i.e., due to fast feedbacks in the climate system, $\lambda\Delta T$), but this study is not concerned with distinguishing between feedback related imbalances ($\lambda\Delta T$) and other unforced imbalances (ε).

We are particularly interested in the fractional Q_{TOA} contribution to decadal scale T change (i.e., how much of a given change in T can be attributable to the net energy flux at the TOA?). This can be estimated by rearranging equation (1) to form the ratio of a given Q_{TOA} flux to the total energy flux necessary for a simulated T change to have occurred,

$$\text{fractional } Q_{TOA} \text{ contribution to } T \text{ change} = \frac{-Q_{TOA}}{Q_{BML} - Q_{TOA}} = \frac{-Q_{TOA}}{C_m \frac{dT}{dt}}. \tag{3}$$

This formulation makes use of conservation of energy and thus any T change that is not caused by Q_{TOA} is attributable to Q_{BML} (which does not require explicit calculation and is treated as a residual). Therefore, a negative (positive) Q_{TOA} flux does not necessarily imply warming (cooling) as Q_{BML} may be of the same sign as Q_{TOA} but with a larger magnitude. In fact, the fractional Q_{TOA} contributions can be positive (if Q_{TOA} enhances T change) or negative (if Q_{TOA} reduces T change).

In reality, a given net energy flux into the Earth's land/atmosphere/ocean mixed layer system may manifest itself in ways other than changing the temperature (e.g., by melting ice), but these terms are relatively small [*Church et al*., 2011] and thus they do not preclude equation (3) from providing a first-order estimate of unforced Q_{TOA} influence on T. The primary uncertainty in equation (3) comes from C_m [*Baker and Roe*, 2009; *Geoffroy et al*., 2012], but our results are robust to various representations of C_m (see supporting information).

3. Q_{TOA} Contribution to Unforced Decadal Scale T Fluctuations

Figure 1 compares mean energy fluxes and surface temperature trends over large decade-scale T warming and T cooling events over the course of the unforced control runs (the two largest-magnitude warming and two largest-magnitude cooling decades were selected from each of the 36 control runs). Warming decades were associated with mean Q_{TOA} of ~ -0.06 W/m^2 (Figure 1f), indicating that the entire climate system tended to experience an increase in energy over these periods. Conversely, cooling decades showed a mean Q_{TOA} of $\sim +0.06$ W/m^2 (Figure 1f), indicating that the climate system tended to lose energy during these periods. This implies that a portion of the energy surplus (deficit) during warming (cooling) decades comes from Q_{TOA} and thus the change in T is not *only* a result of a vertical redistribution of heat within the climate system (this result is supported by the recent study by *Palmer and McNeall* [2014] that shows a positive correlation between unforced decadal T trends and Earth system energy uptake). The surface net upward energy flux (sum of net shortwave, net longwave, latent heat, and sensible heat) shows the same sign and approximate magnitude of Q_{TOA} for both warming and cooling decades (Figure 1e), which indicates that much of the energy surplus (deficit) experienced at the TOA was also experienced at the surface (consistent with the atmosphere having a relatively small heat capacity [*Trenberth*, 2009] compared to the rest of the climate system).

Q_{TOA} was also decomposed into outgoing longwave (OLR) and reflected shortwave (RSW) components. Mean OLR was not significantly different between the warming and cooling decades (Figure 1a) and thus almost all the difference in mean Q_{TOA} was attributable to differences in mean RSW (reduced albedo during warming decades and enhanced albedo during cooling decades, Figure 1b). Linear trends in surface air temperature over the Niño 3 region (5°S–5°N and 150°W–90°W) are of the same sign (Figure 1d), but approximately twice as large as T trends (Figure 1c) indicating that warming (cooling) decades are associated with a transition to a more El Niño (La Niña) like state (on this timescale such variability is attributable more to

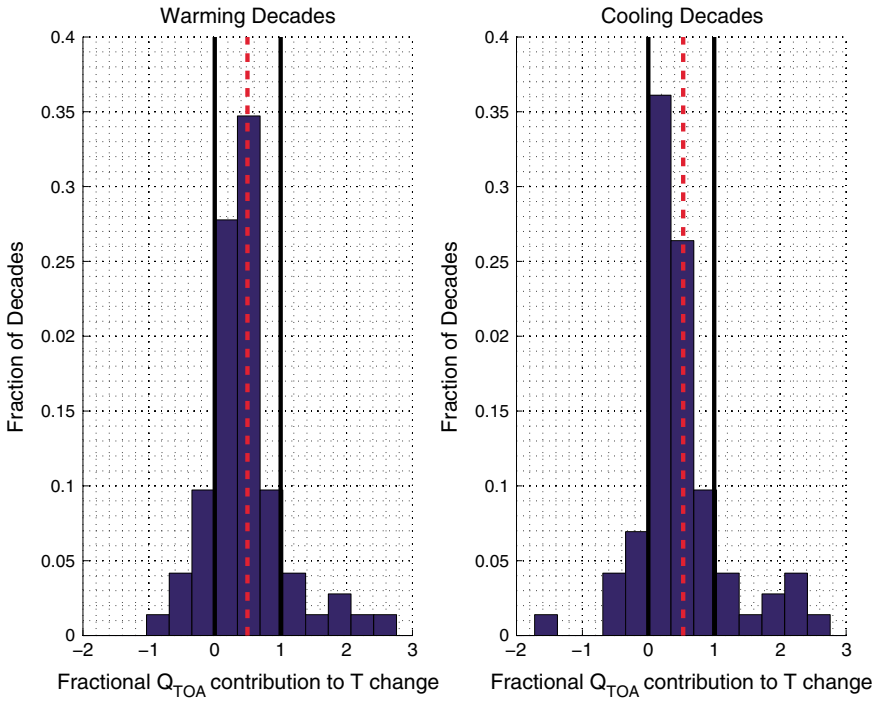

Figure 2. Normalized histograms (pooled across all GCMs) of the fractional Q_{TOA} contribution to the simulated unforced T fluctuations (equation (3)). The solid black lines delineate the 0 and 1 values while the red dashed line indicates the mean of the distribution. For these calculations, Q_{TOA} was the average global flux (in W/m^2) over the simulated decade, and dT/dt was the mean rate of change of T in kelvins/s over the decade (calculated by least squares linear regression).

the Interdecadal Pacific Oscillation (IPO) than to the El Niño–Southern Oscillation (ENSO) [*Power et al*., 1999; *Salinger et al*., 2001]).

The distributions of fractional Q_{TOA} contribution to decadal warming/cooling episodes (equation (3)) are shown in Figure 2. The average fractional Q_{TOA} contributions were similar for both warming and cooling decades (0.5 for warming decades and 0.53 for cooling decades), meaning that about half of the energy flux required for the simulated changes in T is attributable to Q_{TOA} (the average fractional Q_{TOA} contribution to T change ranges from 0.44 to 0.68 depending on how C_m is treated, see supporting information). The range of the fractional Q_{TOA} contribution is large from individual decade to decade with some instances above 1 (13% of warming decades and 15% of cooling decades) and some instances below 0 (15% of warming decades and 13% of decades). A fractional contribution above 1 would imply that during that decade, Q_{TOA} provided more than enough net energy flux for the simulated T change to have occurred and thus Q_{BML} must have countered the effect of Q_{TOA}. On the other hand, an instance below 0 would imply that during that decade, Q_{TOA} worked to suppress the simulated change in T and thus Q_{BML} must have provided more than enough of the necessary energy flux. Most of the decades studied here (72% of both warming and cooling decades) have fractional Q_{TOA} contributions between 0 and 1 indicating that Q_{TOA} and Q_{BML} tend to work cooperatively, both contributing positively to the simulated T change.

4. Change in Energy Flux During Warming and Cooling Decades

The warming and cooling decades in the unforced control runs are associated with significant changes in energy fluxes in both space and time. Figure 3 illustrates the composite global mean behavior of TOA radiation variables, as well as surface net upward energy flux and surface temperature both globally and over the Niño 3 region, while Figure 4 shows the mean spatial behavior of these variables over the same decades. The shading in Figure 3 represents the standard deviation across all decades, while the stippling in Figure 4 shows locations where more than 75% of the simulated decades experienced the same sign of the given

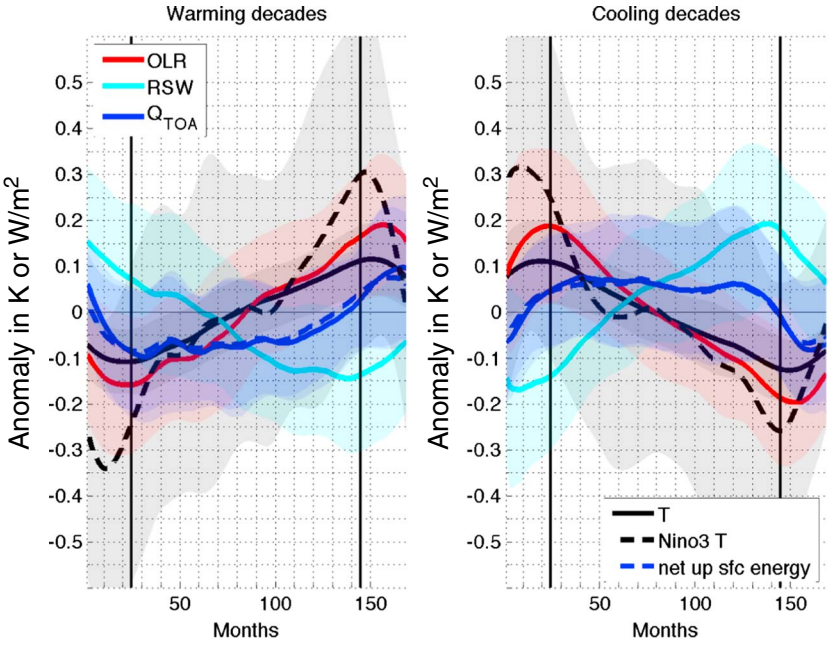

Figure 3. Composite energy flux (Q_{TOA}, RSW, OLR, and surface net upward energy) and surface temperature anomalies (T and surface temperature over the Niño 3 region) over the same warming and cooling decades described in Figures 1 and 2. The shading denotes the standard deviation of each value across all decades. All variables are expressed as anomalies relative to their mean over the entire control run. Fourteen years are shown but calculations in Figures 1, 2, and 4 are only preformed on the decade enclosed by the vertical black lines.

value. The relatively large standard deviations in Figure 3 as well as the relatively small area stippled in Figure 4 indicate that the patterns simulated in individual decades can vary substantially from the mean pattern across all decades.

As was implied by Figure 1, warming (cooling) decades tend to be associated with locally enhanced warming (cooling) over the central equatorial Pacific which implies a shift from negative (positive) phase to positive (negative) phase in the IPO [*Power et al*., 1999; *Salinger et al*., 2001] (Figure 4). The Global Climate Model (GCM) mean warming (cooling) is distributed nearly globally, with notable exceptions over the western Pacific midlatitude regions in both the Northern and Southern Hemispheres (Figure 4), consistent with the typical spatial pattern associated with the IPO [*Power et al*., 1999] and/or the Pacific Decadal Oscillation [*Deser et al*., 2010; *Mantua et al*., 1997]. The warming (cooling) is particularly strong in the high latitudes which may be a result of energy surpluses (deficits) over the tropical Pacific being transferred to the poles through large shifts in meridional atmospheric energy transport [*Trenberth et al*., 2002a; *Trenberth et al*., 2002b].

As T increases (decreases) over the course of the decade, OLR also tends to increase (decrease) globally (Figure 3), which is, to the first order, due to the basic Stefan-Boltzmann response (i.e., "Planck response" or "Blackbody response") of the climate system [*Forster and Taylor*, 2006]. All else being equal, this OLR change would quickly eliminate any initial imbalance in Q_{TOA} and would work to stabilize T. These simulated T changes, however, appear to be sustained, in part, by changes in albedo (of order 0.1%, Figure S7) that work to counteract the changes in OLR (Figure 3). During warming (cooling) decades, the largest decrease (increase) in RSW radiation occurs over the central/eastern equatorial Pacific, off the east coast of Australia and over the Southern Ocean, particularly over the Weddell Sea (Figure 4). In the Pacific, the RSW change displayed in Figure 4 suggests a distinct shift in the location of the South Pacific Convergence Zone which has been noted to occur in conjunction with a phase shift in the IPO [*Folland et al*., 2002].

The RSW and OLR changes are of opposite sign over much of the Earth, consistent with a reorganization of convective cloud regimes in which local RSW changes tend to be cancelled at the TOA by counteracting changes in OLR [*Kato*, 2009; *Kiehl and Ramanathan*, 1990]. The cancellation is not perfect everywhere, however, as warming (cooling) decades are associated with a positive (negative) change in Q_{TOA} over much

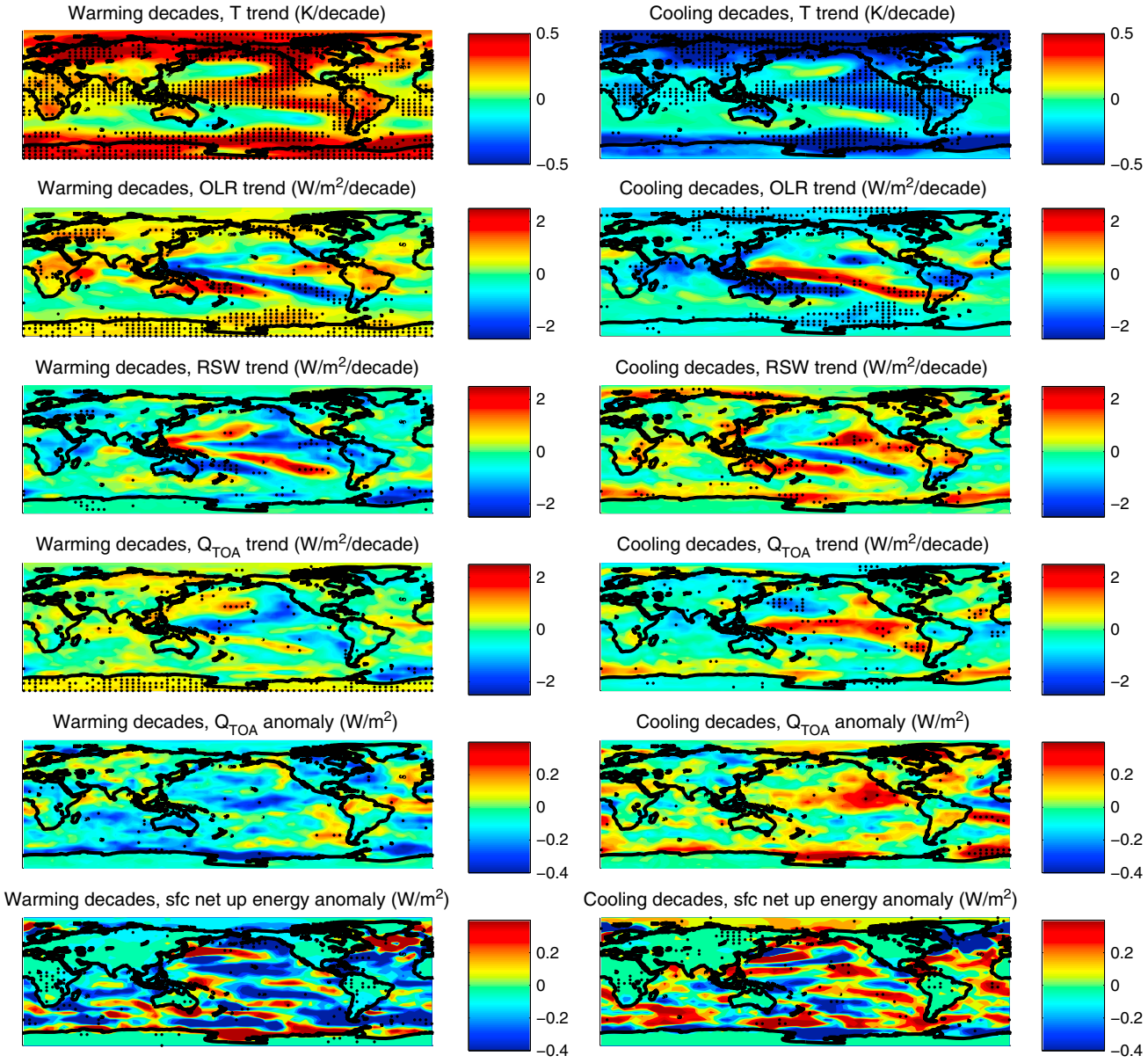

Figure 4. Rates of change and anomalies of energy flux variables and surface temperatures over the same warming and cooling decades discussed in Figures 1–3. Stippling delineates the grid points where over 75% of the decades experienced the same signed value. Additional maps are shown in Figure S6.

of the middle and high latitudes where change in OLR is greater than any counteracting change in RSW. This enhanced (reduced) OLR eventually contributes to the demise of the warming (cooling) period by driving Q_{TOA} from negative (positive) to positive (negative) (Figure 3). However, warming (cooling) periods may be enhanced in both duration and magnitude by reinforcing changes in RSW over the central equatorial and eastern Pacific. In these regions, warming (cooling) surface temperatures tend to be associated with decreased (increased) RSW, which is not fully cancelled by changes in OLR (Figure 4). The reason for this is likely that the eastern equatorial Pacific is characterized by more large-scale atmospheric subsidence, relatively cool surface temperatures and marine stratiform clouds [*Klein and Hartmann*, 1993]. Marine stratiform clouds have a net cooling effect on the surface (i.e., their presence increases RSW more than it reduces OLR) [*Hartmann et al.*, 1992]. Therefore, a breakup of these clouds due to surface warming will reduce RSW without a wholly compensating increase in OLR [*Sun et al.*, 2003; *Wallace et al.*, 1989]. This is consistent with the result that most GCMs exhibit positive cloud feedback primarily due to a

reduction in low clouds when the surface warms [*Soden et al*., 2008]. The lack of complete cancellation between OLR and RSW in the central and eastern Pacific allows for Q_{TOA} to contribute to ENSO via the "shortwave heat flux feedback" [*Bony et al*., 1997], and thus, it is reasonable that it would also play a role in longer timescales as part of the IPO.

5. Discussion and Summary

The present study supports previous work that has attributed a significant component of decadal scale unforced variability in T to low frequency ENSO variability and/or the IPO [*Kosaka and Xie*, 2013; *Meehl et al*., 2011; *Meehl et al*., 2013; *Trenberth and Fasullo*, 2013]. However, our results differ from most previous studies in that we show that energy imbalances at the TOA can enhance unforced T change rather than T change being exclusively due to the redistribution of energy within the climate system. We show that these TOA imbalances come about because albedo changes are able to temporarily counteract the climate system's outgoing longwave (i.e., Stefan-Boltzmann) response to T change. It should be noted that since ENSO and the IPO also affect T via large vertical redistributions of heat (i.e., changes in Q_{BML}) [*Meehl et al*., 2013; *Trenberth et al*., 2002a], the simulated Q_{TOA} imbalances are likely to be dominated by the feedback component ($\lambda\Delta T$) rather than being spontaneously generated by the atmosphere (ε) [*Trenberth et al*., 2010].

It is worthwhile to attempt to interpret the present results in the context of contemporary climate change. From the years 1955 to 2010, 0–2000 m ocean heat content accumulation suggested that the mean Q_{TOA} over this period was ~0.27 W/m^2 (due mostly to external radiative forcings, F) [*Levitus et al*., 2012]. This study has shown that in extreme episodes of decadal scale unforced T change, mean Q_{TOA} imbalances were on the order of ± ~0.06 W/m^2 averaged across all GCMs (the most extreme imbalances observed were ± ~0.2 W/m^2, Figure S4). This would imply that in certain circumstances, unforced variability in Q_{TOA} may have been able to modulate the long-term forced imbalance by ~22% (~74% in the most extreme circumstances) over the course of a given decade. Currently, however, measurements indicate that the energy imbalance at the TOA is between 0.5 and 1.0 W/m^2 [*Abraham et al*., 2013; *Trenberth et al*., 2014]. At this magnitude, unforced Q_{TOA} variability would only be able to modulate the background forced imbalance by ~6–12% (~20–40% in the most extreme circumstances) over the entirety of a given decade.

It is interesting to note that the best available inventories of total climate system heat content suggest that the recent slowdown in T warming has *not* been accompanied by a decrease in the net energy imbalance at the TOA [*Balmaseda et al*., 2013; *Trenberth et al*., 2014]. This indicates that the fractional Q_{TOA} contribution to recent unforced T change might be close to 0% or less (i.e., Q_{BML} may have accounted for 100% or more of the net energy flux necessary for the observed change in T progression to have occurred). Indeed, there is a growing consensus that the recent slowdown in the increase in T has been due to increased heat storage in the ocean below the mixed layer [*Balmaseda et al*., 2013; *England et al*., 2014; *Meehl et al*., 2011; *Meehl et al*., 2013; *Trenberth and Fasullo*, 2013]. The present study indicates that fractional Q_{TOA} contributions to T change below 0% (during cooling decades) are not typical as they occurred in nine out of 72 (12.5%) decades investigated (Figure 2). Therefore, if GCMs correctly simulate the relationship between unforced T change and Q_{TOA}, the current "warming hiatus" may be an aberration in that we should expect most unforced decadal changes in T to be *enhanced* by the Q_{TOA} imbalance.

Because unforced variability in the tropical Pacific appears to be a major driver of decadal scale unforced variability in T and Q_{TOA}, accurate GCM simulation of internal modes such as ENSO are of upmost importance. This is particularly true given that lower frequency modes of variability like the IPO and PDO may depend on accurate simulation of ENSO [*Schneider and Cornuelle*, 2005]. The CMIP5 multimodel ensemble saw an improvement in ENSO simulation over the previous generation of GCMs, particularly in their ability to accurately produce a spectral peak in sea surface temperature variability within the 2–7 year range [*Flato et al*., 2013]. Despite this, many GCMs still have significant biases in their simulation of physical processes (such as deep convection, trade wind strength and clouds) key to ENSO dynamics [*Flato et al*., 2013; *Jiang et al*., 2012]. In particular, the shortwave heat flux feedback associated with ENSO may be critical for the accurate representation of Q_{TOA} variability but it remains poorly simulated in current GCMs [*Bellenger et al*., 2013]. Of particular relevance is the recent study by *England et al*. [2014] which showed that current GCMs do not accurately simulate the magnitude of observed unforced variability in trade wind strength which has

enhanced deep ocean heat uptake (i.e., Q_{BML}) over the recent past. It is quite possible that similar errors may exist when it comes to the simulated relationship between unforced Q_{TOA} and T. For example, the shortwave feedback due to low-level clouds, which this study suggests plays an important role in unforced T variability, has a very large intermodel spread [*Sherwood et al.*, 2014]. Going forward, addressing these issues may lead to improved GCM performance on decadal timescales which would be valuable for "decadal prediction" of climate change on policy relevant timescales [*Meehl et al.*, 2009].

Acknowledgments

We would like to acknowledge Norman Loeb, Jonathan Jiang, and Ana Barros for offering insightful comments on this research. We acknowledge the World Climate Research Programme's Working Group on Coupled Modelling, which is responsible for CMIP, and we thank the climate modeling groups for producing and making available their model output. For CMIP, the U.S. Department of Energy's Program for Climate Model Diagnosis and Intercomparison provides coordinating support and led development of software infrastructure in partnership with the Global Organization for Earth System Science Portals. We would also like to acknowledge the work of Geert Jan van Oldenborgh for providing CMIP5 data at http://climexp.knmi.nl/. This work was partially supported by NSF grant AGS-1147608.

The Editor thanks two anonymous reviewers for their assistance in evaluating this paper.

References

Abraham, J. P., et al. (2013), A review of global ocean temperature observations: Implications for ocean heat content estimates and climate change, *Rev. Geophys.*, *51*, 450–483, doi:10.1002/rog.20022.

Baker, M. B., and G. H. Roe (2009), The shape of things to come: Why is climate change so predictable?, *J. Clim.*, *22*(17), 4574–4589, doi:10.1175/2009JCLI2647.1.

Balmaseda, M. A., K. E. Trenberth, and E. Källén (2013), Distinctive climate signals in reanalysis of global ocean heat content, *Geophys. Res. Lett.*, *40*, 1754–1759, doi:10.1002/grl.50382.

Bellenger, H., E. Guilyardi, J. Leloup, M. Lengaigne, and J. Vialard (2013), ENSO representation in climate models: From CMIP3 to CMIP5, *Clim. Dyn.*, 1–20, doi:10.1007/s00382-013-1783-z.

Bony, S., K.-M. Lau, and Y. C. Sud (1997), Temperature and large-scale circulation influences on tropical greenhouse effect and cloud radiative forcing, *J. Clim.*, *10*, 2055–2077.

Church, J. A., N. J. White, L. F. Konikow, C. M. Domingues, J. G. Cogley, E. Rignot, J. M. Gregory, M. R. van den Broeke, A. J. Monaghan, and I. Velicogna (2011), Revisiting the Earth's sea-level and energy budgets from 1961 to 2008, *Geophys. Res. Lett.*, *38*, L18601, doi:10.1029/2011GL048794.

Deser, C., M. A. Alexander, S.-P. Xie, and A. S. Phillips (2010), Sea surface temperature variability: Patterns and mechanisms, *Annu. Rev. Mar. Sci.*, *2*(1), 115–143, doi:10.1146/annurev-marine-120408-151453.

Dickinson, R. E. (1981), Convergence rate and stability of ocean–Atmosphere coupling schemes with a zero-dimensional climate model, *J. Atmos. Sci.*, *38*(10), 2112–2120, doi:10.1175/1520-0469(1981)038<2112:CRASOO>2.0.CO;2.

England, M. H., S. McGregor, P. Spence, G. A. Meehl, A. Timmermann, W. Cai, A. S. Gupta, M. J. McPhaden, A. Purich, and A. Santoso (2014), Recent intensification of wind-driven circulation in the Pacific and the ongoing warming hiatus, *Nature Clim. Change*, doi:10.1038/nclimate2106. [Available at http://www.nature.com/nclimate/journal/vaop/ncurrent/abs/nclimate2106.html - supplementary-information.]

Flato, G., et al. (2013), Evaluation of climate models, in *Climate Change 2013: The Physical Science Basis, Contribution of Working Group I to the Fifth Assessment Report of the Intergovernmental Panel on Climate Change*, edited by T. F. Stocker et al., chap. 9, Cambridge Univ. Press, Cambridge, U. K., and New York.

Folland, C. K., J. A. Renwick, M. J. Salinger, and A. B. Mullan (2002), Relative influences of the Interdecadal Pacific Oscillation and ENSO on the South Pacific Convergence Zone, *Geophys. Res. Lett.*, *29*(13), 1643, doi:10.1029/2001GL014201.

Forster, P. M. F., and J. M. Gregory (2006), The climate sensitivity and its components diagnosed from Earth radiation budget data, *J. Clim.*, *19*(1), 39–52, doi:10.1175/JCLI3611.1.

Forster, P. M. F., and K. E. Taylor (2006), Climate forcings and climate sensitivities diagnosed from coupled climate model integrations, *J. Clim.*, *19*(23), 6181–6194, doi:10.1175/JCLI3974.1.

Geoffroy, O., D. Saint-Martin, D. J. L. Olivié, A. Voldoire, G. Bellon, and S. Tytéca (2012), Transient climate response in a two-layer energy-balance model. Part I: Analytical solution and parameter calibration using CMIP5 AOGCM experiments, *J. Clim.*, *26*(6), 1841–1857, doi:10.1175/JCLI-D-12-00195.1.

Guemas, V., F. J. Doblas-Reyes, I. Andreu-Burillo, and M. Asif (2013), Retrospective prediction of the global warming slowdown in the past decade, *Nature Clim. Change*, *3*(7), 649–653, doi:10.1038/nclimate1863. [Available at http://www.nature.com/nclimate/journal/v3/n7/abs/nclimate1863.html - supplementary-information.]

Hartmann, D. L., M. E. Ockert-Bell, and M. L. Michelsen (1992), The effect of cloud type of Earth's energy balance: Global analysis, *J. Clim.*, *5*, 1281–1304.

Hasselmann, K. (1976), Stochastic climate models Part I. Theory, *Tellus*, *28*(6), 473–485, doi:10.1111/j.2153-3490.1976.tb00696.x.

Hawkins, E., and R. Sutton (2009), The potential to narrow uncertainty in regional climate predictions, *Bull. Am. Meteorol. Soc.*, *90*(8), 1095–1107, doi:10.1175/2009BAMS2607.1.

Held, I. M., M. Winton, K. Takahashi, T. Delworth, F. Zeng, and G. K. Vallis (2010), Probing the fast and slow components of global warming by returning abruptly to preindustrial forcing, *J. Clim.*, *23*(9), 2418–2427, doi:10.1175/2009JCLI3466.1.

Jiang, J. H., et al. (2012), Evaluation of cloud and water vapor simulations in CMIP5 climate models using NASA "A-Train" satellite observations, *J. Geophys. Res.*, *117*, D14105, doi:10.1029/2011JD017237.

Kato, S. (2009), Interannual variability of the global radiation budget, *J. Clim.*, *22*(18), 4893–4907, doi:10.1175/2009JCLI2795.1.

Kiehl, J. T., and V. Ramanathan (1990), Comparison of cloud forcing derived from the Earth radiation budget experiment with that simulated by the NCAR community climate model, *J. Geophys. Res.*, *95*(D8), 11,679–11,698, doi:10.1029/JD095iD08p11679.

Klein, S. A., and D. L. Hartmann (1993), The seasonal cyle of low stratiform clouds, *J. Clim.*, *6*, 1587–1606.

Kosaka, Y., and S.-P. Xie (2013), Recent global-warming hiatus tied to equatorial Pacific surface cooling, *Nature*, *501*(7467), 403–407, doi:10.1038/nature12534.

Levitus, S., et al. (2012), World ocean heat content and thermosteric sea level change (0–2000 m), 1955–2010, *Geophys. Res. Lett.*, *39*, L10603, doi:10.1029/2012GL051106.

Loeb, N., S. Kato, W. Su, T. Wong, F. Rose, D. Doelling, J. Norris, and X. Huang (2012), Advances in understanding top-of-atmosphere radiation variability from satellite observations, *Surv. Geophys.*, *33*(3–4), 359–385, doi:10.1007/s10712-012-9175-1.

Mantua, N. J., S. R. Hare, Y. Zhang, J. M. Wallace, and R. C. Francis (1997), A Pacific interdecadal climate oscillation with impacts on salmon production, *Bull. Am. Meteorol. Soc.*, *78*(6), 1069–1079, doi:10.1175/1520-0477(1997)078<1069:APICOW>2.0.CO;2.

Meehl, G. A., et al. (2009), Decadal prediction, *Bull. Am. Meteorol. Soc.*, *90*(10), 1467–1485, doi:10.1175/2009BAMS2778.1.

Meehl, G. A., J. M. Arblaster, J. T. Fasullo, A. Hu, and K. E. Trenberth (2011), Model-based evidence of deep-ocean heat uptake during surface-temperature hiatus periods, *Nature Clim. Change*, *1*(7), 360–364. [Available at http://www.nature.com/nclimate/journal/v1/n7/abs/nclimate1229.html - supplementary-information.]

Meehl, G. A., A. Hu, J. M. Arblaster, J. Fasullo, and K. E. Trenberth (2013), Externally forced and internally generated decadal climate variability associated with the interdecadal Pacific oscillation, *J. Clim.*, *26*(18), 7298–7310, doi:10.1175/JCLI-D-12-00548.1.

Palmer, M. D., and D. J. McNeall (2014), Internal variability of Earth's energy budget simulated by CMIP5 climate models, *Environ. Res. Lett.*, *9*(3), 034016.

Power, S., T. Casey, C. Folland, A. Colman, and V. Mehta (1999), Inter-decadal modulation of the impact of ENSO on Australia, *Clim. Dyn.*, *15*(5), 319–324, doi:10.1007/s003820050284.

Salinger, M. J., J. A. Renwick, and A. B. Mullan (2001), Interdecadal Pacific Oscillation and South Pacific climate, *Int. J. Climatol.*, *21*(14), 1705–1721, doi:10.1002/joc.691.

Schneider, N., and B. D. Cornuelle (2005), The forcing of the Pacific Decadal Oscillation, *J. Clim.*, *18*(21), 4355–4373, doi:10.1175/JCLI3527.1.

Sherwood, S. C., S. Bony, and J.-L. Dufresne (2014), Spread in model climate sensitivity traced to atmospheric convective mixing, *Nature*, *505*(7481), 37–42, doi:10.1038/nature12829.

Soden, B. J., I. M. Held, R. Colman, K. M. Shell, J. T. Kiehl, and C. A. Shields (2008), Quantifying climate feedbacks using radiative kernels, *J. Clim.*, *21*(14), 3504–3520, doi:10.1175/2007JCLI2110.1.

Solomon, S., et al. (2007), *Climate Change 2007: The Physical Science Basis, Contribution of Working Group I to the Fourth Assessment Report of the Intergovernmental Panel on Climate Change*, Cambridge Univ. Press, Cambridge, U. K., and New York.

Sun, D., J. T. Fasullo, T. Zhang, and A. Roubicek (2003), On the radiative and dynamical feedbacks over the equatorial Pacific cold tongue, *J. Clim.*, *16*, 2425–2432.

Susskind, J., G. Molnar, L. Iredell, and N. G. Loeb (2012), Interannual variability of outgoing longwave radiation as observed by AIRS and CERES, *J. Geophys. Res.*, *117*, D23107, doi:10.1029/2012JD017997.

Taylor, K. E., R. J. Stouffer, and G. A. Meehl (2011), An overview of CMIP5 and the experiment design, *Bull. Am. Meteorol. Soc.*, *93*(4), 485–498, doi:10.1175/BAMS-D-11-00094.1.

Trenberth, K., and J. Fasullo (2012), Tracking Earth's energy: From El Niño to global warming, *Surv. Geophys.*, *33*(3–4), 413–426, doi:10.1007/s10712-011-9150-2.

Trenberth, K. E. (2009), An imperative for climate change planning: Tracking Earth's global energy, *Curr. Opin. Environ. Sustainability*, *1*(1), 19–27, doi:10.1016/j.cosust.2009.06.001.

Trenberth, K. E., and J. T. Fasullo (2013), An apparent hiatus in global warming?, *Earth's Future*, *1*, 19–32, doi:10.1002/2013EF000165.

Trenberth, K. E., J. M. Caron, D. P. Stepaniak, and S. Worley (2002a), Evolution of El Niño–Southern Oscillation and global atmospheric surface temperatures, *J. Geophys. Res.*, *107*(D8), 4065, doi:10.1029/2000JD000298.

Trenberth, K. E., D. P. Stepaniak, and J. M. Caron (2002b), Interannual variations in the atmospheric heat budget, *J. Geophys. Res.*, *107*(D8), 4066, doi:10.1029/2000JD000297.

Trenberth, K. E., J. T. Fasullo, C. O'Dell, and T. Wong (2010), Relationships between tropical sea surface temperature and top-of-atmosphere radiation, *Geophys. Res. Lett.*, *37*, L03702, doi:10.1029/2009GL042314.

Trenberth, K. E., J. T. Fasullo, and M. A. Balmaseda (2014), Earth's energy imbalance, *J. Clim.*, doi:10.1175/JCLI-D-13-00294.1.

Wallace, J. M., T. P. Mitchell, and C. Deser (1989), The influence of sea-surface temperature on surface wind in the eastern equatorial Pacific: Seasonal and interannual variability, *J. Clim.*, *2*, 1492–1499.

Wielicki, B. A., B. R. Barkstrom, E. F. Harrison, R. B. Lee III, G. L. Smith, and J. E. Cooper (1996), Clouds and the Earth's Radiant Energy System (CERES): An Earth observing system experiment, *Bull. Am. Meteorol. Soc.*, *77*(5), 853–868, doi:10.1175/1520-0477(1996)077<0853:CATERE>2.0.CO;2.

Wigley, T. M. L., and M. E. Schlesinger (1985), Analytical solution for the effect of increasing CO_2 on global mean temperature, *Nature*, *315*(6021), 649–652.

Wigley, T. M. L., and S. C. B. Raper (1990), Natural variability of the climate system and detection of the greenhouse effect, *Nature*, *344*(6264), 324–327.